A Highly Linear Modified Super Source Follower-Based Active Feedback Wideband LNA for Sub-GHz Wireless IoT Application

Euiseong Kim[1], Seokgyu Lee, Deok-Young Kim and Donggu Im[a]
Division of Electronic Engineering, Jeonbuk National University
E-mail : [1]ergle7843@naver.com

***Abstract*—This paper presents a highly linear modified super source follower (SSF)-based active feedback wideband low noise amplifier (LNA) for sub-GHz wireless Internet-of-Things (IoT) applications. To further increase the loop gain and improve both the noise figure (NF) and linearity of the LNA, it is necessary to reduce the output impedance of the voltage follower in the feedback path so that it behaves more like an ideal voltage buffer. To achieve this, the proposed wideband LNA employs an advanced source follower (modified SSF) by combining a flipped voltage follower (FVF) with an SSF, forming a voltage buffer within the feedback path. Two feedback paths are utilized to increase the loop gain and enhance the effective transconductance of the input transistor in the advanced SSF. Additionally, to further increase the loop gain, the LNA output signal is applied to the gate of transistor, which serves as the current source device in the modified SSF within the feedback path. This approach directly reduces the output impedance while improving loop gain, noise performance, and linearity. The proposed LNA was designed using a 130-nm CMOS technology. Experimental results show that the input return loss (S_{11}) is less than −10 dB up to 2 GHz, the power gain (S_{21}) is 21 dB, and the NF is 1.6 dB at 900 MHz. The measured 3-dB bandwidth exceeds 2 GHz, and the input third-order intercept point (IIP3) ranges from −6 dBm to −4 dBm with a two-tone spacing of 20 MHz. The total power consumption is approximately 12.5 mW from a 1.2 V supply.**

***Keywords*—Active feedback, CMOS, flipped voltage follower, sub-GHz, super source follower.**

I. INTRODUCTION

Sub-GHz low power Internet of Things (IoT) systems play a crucial role in enabling reliable, long-range, and energy-efficient wireless communication. By operating in frequency bands below 1 GHz, these systems exhibit reduced signal attenuation and enhanced propagation characteristics, allowing for improved penetration through obstacles such as walls, buildings, and vegetation when compared to higher-frequency counterparts. Consequently, sub-GHz IoT technologies are particularly well suited for wide-area applications, including smart cities, precision agriculture, industrial monitoring, and utility metering. In addition to their favorable propagation properties, sub-GHz IoT systems are characterized by inherently low power consumption. End devices can sustain multi-year operation on limited battery capacity, thereby significantly reducing maintenance requirements and operational costs in large-scale deployments. This energy efficiency is critical for supporting massive IoT scenarios involving thousands to millions of distributed nodes. Overall, sub-GHz IoT systems offer a compelling combination of extended communication range, low energy consumption, and robust link reliability. These features establish them as a key enabler for scalable and sustainable IoT infrastructures.

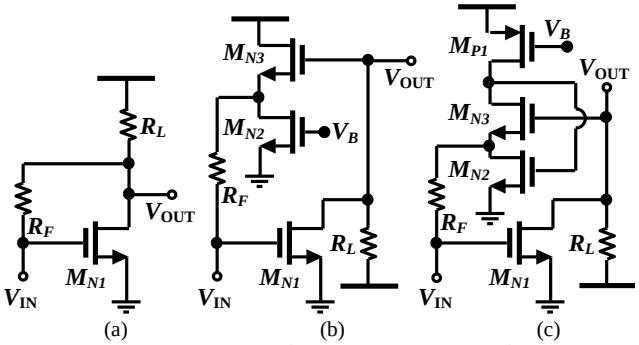

Fig.1. Conventional (a) resistive feedback low noise amplifier (LNA), (b) active feedback LNA using a source follower, (c) active feedback LNA using a flipped voltage follower (FVF).

A wideband low noise amplifier (LNA) is essential in sub-GHz IoT receivers to support multiple regional frequency bands within the sub-1 GHz spectrum, such as 433 MHz, 868 MHz, and 915 MHz [1]-[3]. By providing wideband impedance matching and consistent gain across these frequencies, a broadband LNA enables a single receiver architecture to operate across different regulatory bands without requiring band-specific front-end redesign. In addition, because sub-GHz IoT environments often involve weak signals transmitted over long distances, a wideband LNA with low noise figure (NF) is therefore critical to enhance receiver sensitivity and ensure reliable signal detection. In this paper, a low power, highly linear active feedback LNA employing a modified super source follower (SSF) is proposed for sub-GHz IoT systems.

a. Corresponding author; dgim@jbnu.ac.kr

Manuscript Received Apr. 7, 2026, Revised May 18, 2026, Accepted May 26, 2026

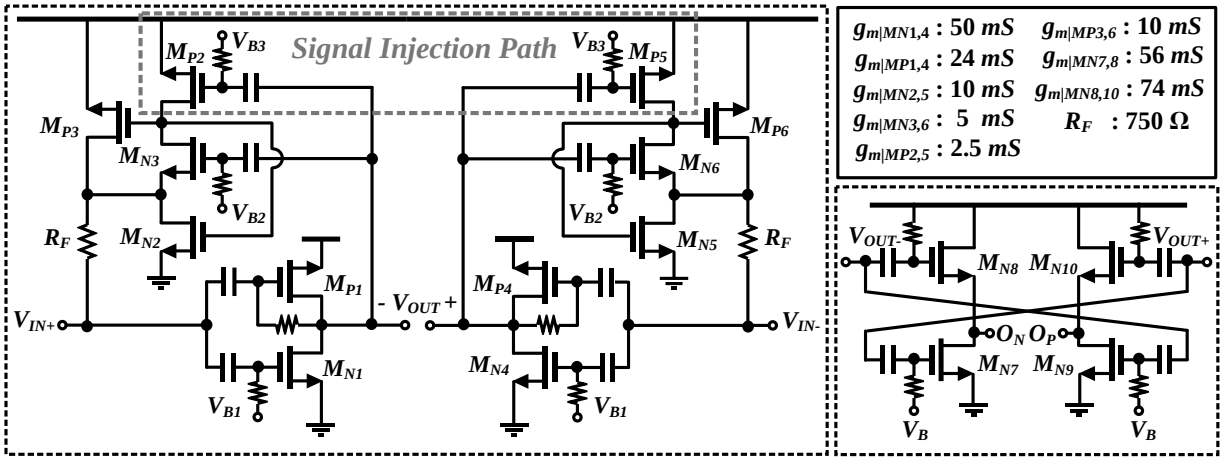

(a) (b)

Fig. 2. (a) Proposed active feedback wideband LNA using the modified super source follower (SSF), (b) its design parameters and output buffer for the measurement.

II. REVIEW OF CONVENTIONAL ACTIVE FEEDBACK LNAS

Compared to a resistive feedback LNA of Fig. 1(a), an active feedback LNA using a source follower shown in Fig. 1(b) is less sensitive to loop gain degradation even when driving a relatively low input impedance load [4]-[6]. The buffer action of the source follower isolates the feedback network from the load, helping maintain more stable loop gain and overall performance. Figure 1(c) presents the conventional active feedback LNA through a flipped voltage follower (FVF) reported in [7]. In case of the voltage follower driving the load impedance R_L, the voltage gain at the output is approximately given by $A_V \approx R_L/(R_{CLO}+R_L) \approx A_V^{\infty} \cdot T_{LOOP}/(1+T_{LOOP})$, where the R_{CLO} is the closed loop output impedance of the voltage follower and the A_V^{∞} is the voltage gain when the loop gain of the voltage follower is close to infinity, and the T_{LOOP} is the loop gain of the voltage follower. Because the A_V^{∞} is 1, the loop gain of the voltage follower is defined as R_L/R_{CLO} [8]. This means that the smaller closed loop output impedance of the voltage follower gives the better linearity, because harmonic distortions are reduced by a factor of loop gain. Using a FVF instead of a conventional source follower further reduces the output impedance of the follower. This enables the use of a larger feedback resistor while maintaining the same input impedance matching condition, thereby further increasing the loop gain and improving the NF of the LNA. As a result, both the linearity and noise performance are enhanced. To achieve additional improvement in NF and linearity, the output impedance of the voltage follower in the feedback path should be minimized so that it more closely approximates an ideal voltage buffer.

III. DESIGN OF PROPOSED ACTIVE FEEDBACK LNA

Figure 2(a) shows the proposed active feedback wideband LNA using the modified source follower. In general, in feedback amplifiers, the noise contribution of the input transistor is dominant. Therefore, to minimize NF, it is desirable to maximize the transconductance (g_m) of the input transistor (M_{N1} and M_{P1}) within the given power consumption and bandwidth constraints. The CMOS inverter topology has been widely used in the design of high-frequency amplifiers due to its high gain, low power consumption, and simple hardware configuration [9]-[10]. The effective transconductance can be easily enhanced through the current-reuse technique. Consequently, the main amplification stage of the proposed LNA is based on a CMOS inverter structure. A high resistance is connected between the gate and drain nodes of the inverter to stabilize the DC operating point.

As is well known, the FVF and SSF are improved versions of the conventional source follower, which have smaller output impedance and better linearity under the same power dissipation. As shown in Fig. 2, the proposed wideband LNA adopts more advanced source follower (modified SSF) by combining FVF and SSF as a voltage buffer within the feedback path. Two feedback paths (M_{N2} and M_{P3}) increase the loop gain, and, as a result, enhance the effective transconductance (g_{mn3}) of the input transistor M_{N3} in the modified SSF. This reduces its output impedance and directly improves the loop gain, noise, and linearity performances. Additionally, to further increase the loop gain, the LNA output signal is applied to the gate of M_{P2}, which serves as the current source device in the modified SSF within the feedback path.

The loop gain of the proposed LNA, when the 50-Ω source resistance is not loaded, can be calculated as follows:

$$T_{LOOP} \approx (g_{mN1} + g_{mP1})(r_{ON1} \parallel r_{OP1})(1 + \frac{g_{mP2}}{g_{mN3}}) \quad (1)$$

where g_{mNi} and g_{mPi} are the transconductance of NMOS M_{Ni} and PMOS M_{Pi}, and r_{ONi} and r_{OPi} are the output resistance of M_{Ni} and M_{Pi}, respectively. The input impedance (R_{IN}) of the proposed LNA can be approximately described as

$$R_{IN} = \frac{R_F + R_{OUT}^{*}}{1+T_{LOOP}} \quad (2)$$

where R_{OUT}^{*} denotes the output impedance seen at the output

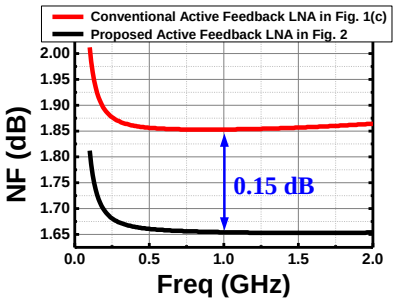

Fig. 3. Comparison of the simulated NF between the conventional active feedback LNA in Fig. 1(c) and the proposed active feedback LNA in Fig. 2.

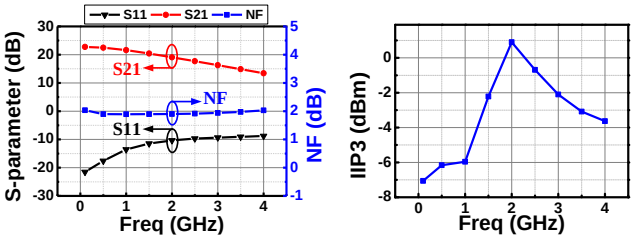

(a) (b)

Fig. 4. Post-layout simulated (a) power gain (S_{21}), input return loss (S_{11}), and noise figure (NF), and (b) input-referred third-order intercept point (IIP3) of the proposed LNA.

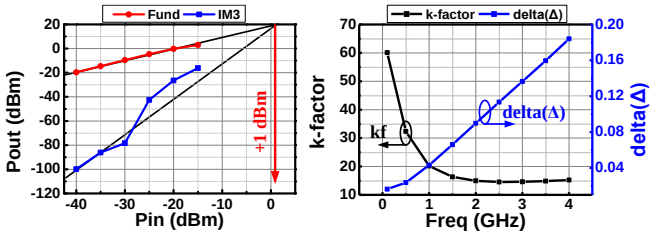

(a) (b)

Fig. 5. Post-layout simulated (a) IIP3 result, shown as an input power versus output power graph, (b) stability factor (K) and auxiliary factor (Δ) of the proposed LNA.

node (i.e., the source of M_{N3}) of the proposed modified SSF. In this design, R_{OUT}^* are T_{LOOP} are approximately 5.7 Ω and 12.6, respectively, and R_F is set to 750 Ω, resulting in an R_{IN} of 55.57 Ω. It is well known that the dominant noise contribution of the feedback LNA comes from input transconductance stage and feedback resistor R_F [11]-[12]. Assuming that all noise sources are not correlated and the input impedance is well matched to source resistance (R_S) of 50 Ω, the excess noise factor (EF) corresponding to thermal noise contribution from M_{N1}, M_{P1}, and R_F are calculated as

$$EF_{MN1} \approx \frac{\gamma}{\alpha} \frac{g_{mN1}}{R_S (g_{mN1} + g_{mP1})^2} \quad (3)$$

$$EF_{MP1} \approx \frac{\gamma}{\alpha} \frac{g_{mP1}}{R_S (g_{mN1} + g_{mP1})^2} \quad (4)$$

$$EF_{R_F} \approx \frac{R_S R_F}{(R_F + R_S)^2}, \quad (5)$$

where γ/a is the bias dependent channel thermal noise coefficient of the transistor. The total noise factor (F_{tot}) of the LNA is approximately given as $1+EF_{MN1}+EF_{MP1}+EF_{RF}$. From (3)-(5), it can be observed that, under the input

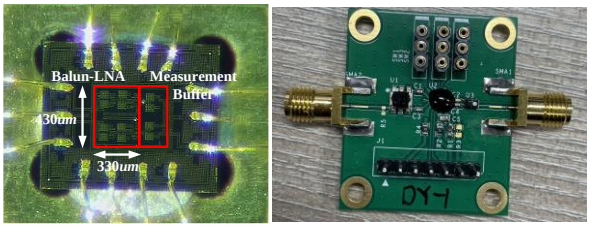

(a) (b)

Fig. 6. Photographs of (a) fabricated chip and (b) measurement board.

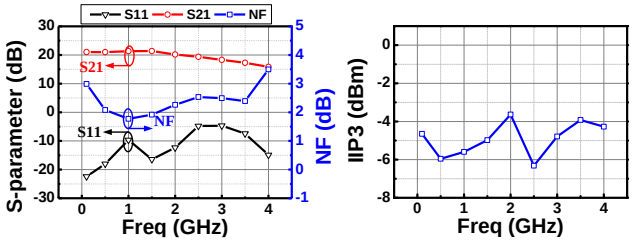

(a) (b)

Fig. 7. Measured (a) S_{21}, S_{11}, and NF, and (b) IIP3 of the proposed LNA.

TABLE I. Measurement Summary and Comparison with Previous Works

	[13]	[14]	[15]	[16]	This Work
Frequency (GHz)	0.13-0.93	0.4-2.2	0.47-3.3	0.02-2	0.1 - 2.25
S_{21} (dB)	19.6	19.8	22	18.5	21
S_{11} (dB)	<-10	<-10	<-10	<-15	< -10
NF (dB)	3.6-5	2.0-2.5	2.57-3.5	2.5-3.5	1.8-3
IIP3 (dBm)	-7.5	-5	2.81	4.2	-3.6
[1]Balun Functionality	Yes	No	Yes	No	Yes
Power (mW)	3 @1.8V	29 @1.2V	12.5 @1.5V	4.1 @1V	12.5 @1.2V
CMOS (nm)	180	65	65	28	130
[2]FoM	2.0	1.0	3.5	5.2	3.8

[1]Balun functionality denotes single-to-differential conversion,
[2]FOM=Gain[lin]*BW[GHz] /{(NF[lin]-1)*P[mW]}

impedance matching condition, the NF of the LNA can be reduced by increasing the g_m of the input transistors M_{N1} and M_{P1}, as well as the feedback resistance R_F.

Figure 3 presents the comparison result of simulated NF between the conventional active feedback LNA in Fig. 1(c) and the proposed active feedback LNA in Fig. 2. Under the same input impedance matching and power consumption conditions, the proposed active feedback LNA employing the modified SSF achieves higher loop gain and lower output resistance (R_{OUT}^*) than its FVF-based counterpart. As a result, R_F can be increased from 450 Ω to 750 Ω, leading to a 0.15 dB reduction in the NF of the LNA.

Figure 4 shows the post-layout simulation results of power gain (S_{21}), input return loss (S_{11}), NF, and input-referred third-order intercept point (IIP3) of the proposed LNA. Although the proposed LNA circuit targets Sub-GHz IoT applications, the performance is reported up to the 4 GHz band because bandwidth is an important parameter for inductor-less feedback LNAs. The S_{21} exhibits a relatively high gain of more than 14 dB up to 4 GHz. The NF is maintained between 1.8 dB and 2 dB. In addition, the S_{11} remains below approximately −10 dB, indicating that the input impedance is well matched to source resistance (R_S) over a wide bandwidth. The simulated IIP3 ranges from -7

dBm to +1 dBm over the whole operating frequency band. Figure 5(a) presents the post-layout simulated IIP3 result, shown as an input power versus output power graph, of the proposed LNA. For the IIP3 simulation, the operating frequency was set to 2 GHz, and the two-tone spacing was set to 20 MHz. In order to verify the stability of the LNA, the stability factor K and auxiliary factor Δ are plotted as shown in Fig. 5(b). Because K is greater than 1 and Δ is less than 1 over the operating frequency band, the proposed LNA remains stable.

IV. EXPERIMENTAL RESULTS

The proposed LNA was implemented in a 0.13-μm CMOS process. Figure 6 shows photographs of the fabricated chip and the measurement board. The LNA was measured using a chip-on-board (COB) package on an FR4 substrate, and the chip area is approximately 0.14 mm², excluding the on-chip measurement buffer and I/O pads. The total power consumption of the LNA, excluding the output buffer, is 12.5 mW from a 1.2 V supply. At the input, an off-chip balun with a turn ratio of 1:$\sqrt{2}$ converts the 50-Ω single-ended source resistance to a 100-Ω differential impedance. At the output, an off-chip balun with a turn ratio of 1:1 is used for differential-to-single-ended conversion. The measurement output buffer shown in Fig. 2(b) is employed to characterize the performance of the LNA core while driving measurement equipment with a 50-Ω termination, such as a vector network analyzer and a spectrum analyzer. The measurement buffer was biased with sufficient current to ensure that its performance does not affect the LNA core. The signal losses caused by the input/output transmission lines and external input/output transformers were de-embedded from the measured S_{21} and NF.

Figure 7(a) presents the measured S_{21}, S_{11}, NF, and IIP3 of the complete LNA. The S_{11} is less than -10 dB up to 2.25 GHz, and S_{21} and NF are 21 dB and 1.8 dB at 900 MHz, respectively. However, in the low-frequency region, the NF slightly degrades due to the effect of flicker noise. The measured 3-dB bandwidth of the amplifier exceeds 2 GHz. Figure 7(b) shows the measured IIP3 of the LNA. Two-tone spacing is set to equal 20 MHz. The measured IIP3 ranges from -6 dBm to -3.6 dBm.

Table I summarizes the experimental results and compares them with those of conventional wideband LNAs. Compared with the state-of-the-art LNAs listed in Table I, the proposed LNA achieves a relatively lower NF and shows a similar figure-of-merit (FoM).

V. CONCLUSIONS

A highly linear modified SSF-based active feedback wideband LNA is implemented for sub-GHz wireless IoT applications. By adopting an advanced source follower (modified SSF) by combining a FVF with an SSF, forming a voltage buffer within the feedback path, the proposed active feedback LNA enhances the loop gain and increases the feedback resistance while maintaining the same input impedance matching. This directly results in higher linearity and lower NF compared to the conventional active feedback LNAs.

ACKNOWLEDGMENT

This work was supported by the Ministry of Education (MOE) and the Jeonbuk State. Republic of Korea, under Grant 2026-RISE-13-JBU. The chip fabrication and EDA tool were supported by the IC Design Education Center (IDEC), Korea.

REFERENCES

[1] P. B. T. Huynh, J. -H. Kim and T. -Y. Yun, "Dual-Resistive Feedback Wideband LNA for Noise Cancellation and Robust Linearization," in *IEEE Transactions on Microwave Theory and Techniques*, vol. 70, no. 4, pp. 2224-2235, April 2022.

[2] S. Kim and K. Kwon, "A 50-MHz–1-GHz 2.3-dB NF Noise-Cancelling Balun-LNA Employing a Modified Current-Bleeding Technique and Balanced Loads," in *IEEE Transactions on Circuits and Systems I: Regular Papers*, vol. 66, no. 2, pp. 546-554, Feb. 2019.

[3] J. Kim and J. Silva-Martinez, "Wideband Inductorless Balun-LNA Employing Feedback for Low-Power Low-Voltage Applications," in *IEEE Transactions on Microwave Theory and Techniques*, vol. 60, no. 9, pp. 2833-2842, Sept. 2012.

[4] D. Im, H. -T. Kim and K. Lee, "A CMOS Resistive Feedback Differential Low-Noise Amplifier With Enhanced Loop Gain for Digital TV Tuner Applications," in *IEEE Transactions on Microwave Theory and Techniques*, vol. 57, no. 11, pp. 2633-2642, Nov. 2009.

[5] J. Borremans, P. Wambacq, C. Soens, Y. Rolain and M. Kuijk, "Low-Area Active-Feedback Low-Noise Amplifier Design in Scaled Digital CMOS," in *IEEE Journal of Solid-State Circuits*, vol. 43, no. 11, pp. 2422-2433, Nov. 2008

[6] T. Chang, J. Chen, L. A. Rigge and J. Lin, "ESD-Protected Wideband CMOS LNAs Using Modified Resistive Feedback Techniques With Chip-on-Board Packaging," in *IEEE Transactions on Microwave Theory and Techniques*, vol. 56, no. 8, pp. 1817-1826, Aug. 2008.

[7] Mizuno, Shunta, Fumiya Naito, and Makoto Nakamura. "Bandwidth enhancement technique for TIA using flipped voltage follower." *IEICE Electronics Express* 14.10 (2017): 20170310-20170310.

[8] D. Im, H. Kim and K. Lee, "A Broadband CMOS RF Front-End for Universal Tuners Supporting Multi-Standard Terrestrial and Cable Broadcasts," in *IEEE Journal of Solid-State Circuits*, vol. 47, no. 2, pp. 392-406, Feb. 2012

[9] Razavi, Behzad. "Fifty applications of the CMOS inverter—Part 1 [The Analog Mind]." *IEEE Solid-State Circuits Magazine* 16.3, 7-14, 2024.

[10] Bae W, “CMOS Inverter as Analog Circuit: An

overview.” in *Journal of Low Power Electronics and Applications*, 9(3), 26, 2019.
[11] B. G. Perumana, J. -H. C. Zhan, S. S. Taylor, B. R. Carlton and J. Laskar, "Resistive-Feedback CMOS Low-Noise Amplifiers for Multiband Applications," in *IEEE Transactions on Microwave Theory and Techniques*, vol. 56, no. 5, pp. 1218-1225, May 2008.
[12] Lee, M. H., & Kwon, K. D. “A 2.4 GHz Low Power Low-IF Receiver Employing OOK and FSK Dual-Mode Demodulator for IoT Applications.” in *Journal of Integrated Circuits and Systems*, *7*(4), 12-16. 2021.
[13] S. Tiwari and J. Mukherjee, "An Inductorless Wid eband Gm-Boosted Balun LNA With nMOS-pMOS Configuration and Capacitively Coupled Loads for Sub-GHz IoT Applications," in *IEEE Transactions o n Circuits and Systems II: Express Briefs*, vol. 68, no. 10, pp. 3204-3208, Oct. 2021.
[14] S. S. Regulagadda, B. D. Sahoo, A. Dutta, K. Y. Varma and V. S. Rao, "A Packaged Noise-Canceling High-Gain Wideband Low Noise Amplifier," in *IEEE Transactions on Circuits and Systems II: Express Briefs*, vol. 66, no. 1, pp. 11-15, Jan. 2019.
[15] B. Shirmohammadi and M. Yavari, "A Linear Wid eband CMOS Balun-LNA With Balanced Loads," i n *IEEE Transactions on Circuits and Systems II: E xpress Briefs*, vol. 69, no. 3, pp. 754-758, March 2 022.
[16] A. Bozorg and R. B. Staszewski, "A 20 MHz–2 GHz Inductorless Two-Fold Noise-Canceling Low-Noise Amplifier in 28-nm CMOS," in *IEEE Trans actions on Circuits and Systems I: Regular Papers*, vol. 69, no. 1, pp. 42-50, Jan. 2022.

Euiseong Kim received the B.S. degrees from the Division of Electronic Engineering, Sejong University, Seoul, South Korea, in 2024, where he is currently pursuing the M.S. degree from Jeonbuk National University (JBNU), Jeonju, South Korea. His research during the M.S. course has focused on low-power reconfigurable intelligent surface (RIS), multiband low noise amplifiers (LNAs), and the co-design of LNAs and PAs in CMOS RF front-end circuits.

Seokgyu Lee received the B.S. degree from the Division of Electronic Engineering, Jeonbuk National University (JBNU), Jeonju, South Korea, in 2025, where he is currently pursuing the M.S. degree. His research during the M.S. course has focused on PVT-compensated reconfigurable intelligent surface (RIS) and wideband low noise amplifiers (LNAs) for CMOS RF front-end circuits.

Deok-Young Kim received the B.S. and MS degrees from the Division of Electronic Engineering, Jeonbuk National University (JBNU), Jeonju, South Korea, in 2024 and 2026, respectively. he is currently with Nextwill, Daejeon, South Korea. His research during the M.S. course was focused on low-power IoT CMOS front-end circuits, including wideband low noise amplifiers (LNAs), mixers, active polyphase filters, and low-output-impedance voltage buffers.

Donggu Im received the B.S., M.S., and Ph.D. degrees in electrical engineering and computer science from the Korea Advanced Institute of Science and Technology (KAIST), Daejeon, Korea, in 2004, 2006, and 2012, respectively. From 2006 to 2009, he was an Associate Research Engineer with LG Electronics, Seoul, Korea, where he was involved in the development of universal analog and digital TV receiver ICs. From 2012 to 2013, he was a Post-Doctoral Researcher with KAIST, where he was involved in the development of the first RF SOI CMOS technology in Korea with SOI business team in National NanoFab Center (NNFC), Daejeon, Korea. In 2013, he joined the Texas Analog Center of Excellence (TxACE), Department of Electrical Engineering, University of Texas at Dallas, as a Research Associate, where he developed ultra-low-power CMOS radios with adaptive impedance tuning circuits. In 2014, he joined the Division of Electronic Engineering, Jeonbuk National University, Jeollabuk-do, Korea, and is now a Professor. His research interests are CMOS analog/RF/mm-wave ICs and system design.